

# Energy Dependent Isospin Asymmetry in Mean-Field Dynamics

T. Gaitanos, M. Kaskulov

*Institut für Theoretische Physik, Universität Giessen, D-35392 Giessen, Germany*

---

## Abstract

The Lagrangian density of relativistic mean-field (RMF) theory with non-linear derivative (NLD) interactions is applied to isospin asymmetric nuclear matter. We study the symmetry energy and the density and energy dependences of nucleon selfenergies. At high baryon densities a soft symmetry energy is obtained. The energy dependence of the isovector selfenergy suppresses the Lane-type optical potential with increasing energy and predicts a  $\rho$ -meson induced mass splitting between protons and neutrons in isospin asymmetric matter.

*Keywords:* relativistic hydrodynamics, non-linear derivative model, isospin asymmetric matter, equation of state, symmetry energy, optical potential.

PACS numbers: 21.65.Cd, 21.65.Mn, 25.70.-z

---

## 1. Introduction

The study of isospin asymmetric nuclear matter is closely related to a few issues which are presently the subjects of ongoing theoretical and experimental researches. At first, the isospin dependence of the nuclear equation of state (EoS) shows up in the density dependence of the symmetry energy. A quantity which drives the structure of neutron rich nuclei and at supra-high densities the physics of supernovae explosions and the structure of compact neutron stars [1, 2]. For instance, the stiffness [3] of the symmetry energy is directly related to the proton-fraction in  $\beta$ -equilibrated neutron stars, which is limited by the onset of the URCA-process [4]. However, the symmetry energy is empirically known up to saturation densities, where it can be determined in nuclear structure studies from Giant and Pigmy resonances and from neutron skin thickness [5]. In the laboratory the symmetry energy can be explored in heavy ion collisions, where the knowledge of the high density EoS is mandatory [6, 7] for the description of the collision dynamics [8, 9, 10, 11, 12, 13] within transport theory [14, 15]. Different heavy ion observables, *e.g.*, collective transverse (in-plane) and elliptic (out-of-plane) flows [16] of particles and/or light fragments, as well as subthreshold strangeness production [17] are sensitive to the stiffness of the EoS. Furthermore, the isospin tracing [18], isoscaling [19], collective isospin flows [20, 21, 22, 23] and isospin ratios of produced mesons [24, 25, 26, 27] represent plausible tools to constrain the isovector EoS at high densities and energies. Moreover, heavy ion collisions allow to probe not only the density of created matter, but also the energy dependence of the nuclear potential [28, 29, 30].

Theoretically, the density and energy dependence of the isovector EoS beyond the saturation density is still controversial. In non-relativistic Skyrme models both possibilities of a soft and a stiff symmetry energies [1, 2, 21, 22] can be obtained. In the RMF models the symmetry energy is determined by the Lorentz-structure of the isovector potential [1], which is described by the vector-isovector  $\rho$ -field, or by  $\rho$ - and an attractive scalar  $\delta$ -fields [31, 32]. In both cases, the symmetry energy rises with increasing baryon density leading to a stiff isovector EoS at high densities. The models with density dependent (DD) couplings [33, 34, 35, 36] predict a soft symmetry energy [37], while the Dirac-Brueckner-Hartree-Fock (DBHF) calculations [38, 39] and other RMF models with complementary exchange (Fock) terms (density-dependent relativistic Hartree-Fock (RHF) [40, 41]) favour again a stiff one.

Concerning the energy dependence, the Schrödinger equivalent optical potential in symmetric matter is well known phenomenologically [42]. However, different empirical analyses give different predictions for the energy dependence of isovector Lane-potential [43, 44, 45, 46, 47]. The microscopic DBHF [38] and BHF [48, 49] models predict a rather constant optical potential at low momenta with a strong decrease at high energies. In Skyrme approaches both cases of a strong increase and a strong decrease of the Lane-potential as a function of energy can be realized [2]. The DD models do not contain any explicit energy dependence, except if one modifies the original DD formalism [33, 34] with additional interaction terms [37], however, with the cost of additional parameters. Note that, the energy dependence of the optical potential has been so far a crucial problem in standard RMF, where the energy dependence appears only due to relativistic effects.

Another question concerns the quasi-particle properties of nucleons in the nuclear matter. The isospin-dependent forces may result in a splitting between the in-medium masses of protons and neutrons which can strongly influence the dynamics in heavy-ion collisions [21, 22]. However, it is still under debate, whether  $m_n^* < m_p^*$  or  $m_n^* > m_p^*$  holds in neutron rich matter. In non-relativistic approaches the in-medium particle mass is described through the energy dependence of the real part of the phenomenological mean-field [50]. Again, the Skyrme-like interactions predict both possibilities [2] for the non-relativistic in-medium mass [50]. In relativistic models the in-medium dependence of the particle mass arises from the Lorentz-scalar character of the relativistic mean-field, i.e., from the scalar selfenergy [50]. It is often denoted as "effective mass" or "Dirac mass", and these definitions we will use in this work. As in the non-relativistic case, same situation holds for the DBHF models where some calculations predict for the Dirac mass  $m_n^* < m_p^*$  [38] and others  $m_n^* > m_p^*$  [51, 52]. In RMF models the mass splitting is merely fixed by the Lorentz structure of the isovector mean-field. Due to the Lorentz-vector character of the  $\rho NN$ -interaction the minimal  $\sigma\omega\rho$ -models do not generate any in-medium mass splitting, except if one in addition introduces the Lorentz-scalar  $\delta$ -field in the isovector channel [31, 32], or if one includes explicitly exchange (Fock) terms in the relativistic formalism [40, 41]. Including the  $\delta$ -field one gets  $m_n^* < m_p^*$ , while in the RHF models both cases  $m_n^* \gtrless m_p^*$  are possible. So far these were the only possibilities to generate the mass splitting in the relativistic mean field theory [31, 32, 37, 40, 41].

In this work we study the isovector interactions in asymmetric nuclear matter. Our

studies are based on the non-linear derivative (NLD) model to RMF proposed in [53]. This approach describes remarkably well the bulk properties of nuclear matter and, in particular, the density dependence of the nuclear EoS and the energy dependence of the proton-nucleus [53] as well as the antiproton-nucleus Schrödinger equivalent optical potentials [54]. The present paper is organized as follows. In Section 2 we briefly outline the NLD model. In Section 3 the approach is applied to isospin symmetric and isospin asymmetric nuclear matter. The numerical realization and details of the calculations are described in Section 4. The results and discussions are presented in Section 5. We finally end up with the summary in Section 6.

## 2. Non-Linear Derivative (NLD) Model

The NLD approach is based on the Lagrangian density of relativistic hydrodynamics (RHD) [55, 56] and describes the in-medium interaction of nucleons through the exchange of auxiliary scalar-isoscalar  $\sigma$ , vector-isoscalar  $\omega^\mu$  and vector-isovector  $\vec{\rho}^\mu$  meson fields. The Lagrangian density is given by

$$\begin{aligned} \mathcal{L} = & \frac{1}{2} [\bar{\Psi} i \gamma_\mu \partial^\mu \Psi - (i \partial^\mu \bar{\Psi}) \gamma_\mu \Psi] - \bar{\Psi} \Psi m \\ & - \frac{1}{2} m_\sigma^2 \sigma^2 + \frac{1}{2} \partial_\mu \sigma \partial^\mu \sigma + \frac{1}{2} m_\omega^2 \omega_\mu \omega^\mu - \frac{1}{4} F_{\mu\nu} F^{\mu\nu} + \frac{1}{2} m_\rho^2 \vec{\rho}_\mu \vec{\rho}^\mu - \frac{1}{4} \vec{G}_{\mu\nu} \vec{G}^{\mu\nu} \\ & + \mathcal{L}_{int} \quad , \end{aligned} \quad (1)$$

where the first two terms describe the (symmetrized) Lagrangian for the nucleon field  $\Psi = (\Psi_p, \Psi_n)^T$  with bare mass  $m$  and the second line contains the standard Lagrangian densities for  $\sigma$ ,  $\omega^\mu$  and  $\vec{\rho}^\mu$  fields with masses  $m_\sigma$ ,  $m_\omega$  and  $m_\rho$ , respectively. The strength tensors are defined as  $F^{\mu\nu} = \partial^\mu \omega^\nu - \partial^\nu \omega^\mu$  and  $\vec{G}^{\mu\nu} = \partial^\mu \vec{\rho}^\nu - \partial^\nu \vec{\rho}^\mu$  for the vector-isoscalar and vector-isovector fields, correspondingly.

In Eq. (1) the last term  $\mathcal{L}_{int}$  contains the interaction between the meson and nucleon fields. In the conventional RHD [55, 56] the meson fields couple to the nucleons via the corresponding Lorentz structures  $\bar{\Psi} \Psi \sigma$ ,  $-\bar{\Psi} \gamma^\mu \Psi \omega_\mu$  and  $-\bar{\Psi} \gamma^\mu \vec{\tau} \Psi \vec{\rho}_\mu$ . Such minimal Walecka-type interactions describe successfully the static properties of nuclear matter around saturation density. However, they are not sufficient for the description of dynamical situations which occur in nucleon-nucleus and heavy-ion collisions, where this minimal model results in a wrong energy dependence of the mean-field. This has been a crucial problem of the RMF models which already attracted much attention in the past [30, 37, 57]. A possible solution to this problem has been suggested in [28], where momentum-dependent form factors which suppress the high momentum components of fields were introduced. This idea has been followed in the NLD model [53] where it was generalized in a manifestly covariant way.

The NLD interaction Lagrangian introduces the non-linear derivative terms into the conventional RHD meson-nucleon vertices. In particular, the Lagrangian density depends on higher-order partial derivatives of the nucleon field  $\Psi$

$$\mathcal{L}_{int} \equiv \mathcal{L}(\Psi, \partial_\alpha \Psi, \partial_\alpha \partial_\beta \Psi, \dots, \bar{\Psi}, \partial_\alpha \bar{\Psi}, \partial_\alpha \partial_\beta \bar{\Psi}, \dots) \quad (2)$$

with the symmetrized meson-nucleon interactions given by ( $\tau$  denotes the isospin operator)

$$\begin{aligned}\mathcal{L}_{int} = & \frac{g_\sigma}{2} \left[ \bar{\Psi} \overleftarrow{\mathcal{D}} \Psi \sigma + \sigma \bar{\Psi} \overrightarrow{\mathcal{D}} \Psi \right] \\ & - \frac{g_\omega}{2} \left[ \bar{\Psi} \overleftarrow{\mathcal{D}} \gamma^\mu \Psi \omega_\mu + \omega_\mu \bar{\Psi} \gamma^\mu \overrightarrow{\mathcal{D}} \Psi \right] \\ & - \frac{g_\rho}{2} \left[ \bar{\Psi} \overleftarrow{\mathcal{D}} \gamma^\mu \vec{\tau} \Psi \vec{\rho}_\mu + \vec{\rho}_\mu \bar{\Psi} \vec{\tau} \gamma^\mu \overrightarrow{\mathcal{D}} \Psi \right] \quad ,\end{aligned}\quad (3)$$

with obvious notations for the fields and their couplings. The new operator  $\mathcal{D}$  acts on the nucleon fields and is the generic non-linear function of partial derivatives. In the model of Ref. [53] a simple exponential cut-off function has been assumed

$$\overrightarrow{\mathcal{D}} := \exp \left( \frac{-v^\alpha i \overrightarrow{\partial}_\alpha + m}{\Lambda} \right) = \sum_{n=0}^{\infty} \frac{(-v^\alpha i \overrightarrow{\partial}_\alpha / \Lambda)^n}{n!} e^{m/\Lambda} , \quad (4)$$

$$\overleftarrow{\mathcal{D}} := \exp \left( \frac{i \overleftarrow{\partial}_\alpha v^\alpha + m}{\Lambda} \right) = \sum_{n=0}^{\infty} \frac{(i \overleftarrow{\partial}_\alpha v^\alpha / \Lambda)^n}{n!} e^{m/\Lambda} . \quad (5)$$

In Eqs. (4) and (5)  $v^\alpha$  denotes an auxiliary dimensionless 4-vector and  $\Lambda$  stands for the cut-off parameter. A way to realize the meaning of the cut-off function is the presence of the momentum (or energy) dependent form factors in the one-boson-exchange models, which cut the high energy behaviour of the meson-exchange vertices [58, 59]. Furthermore, in the limiting case of  $\Lambda \rightarrow \infty$  the standard RHD (or Walecka) model is retained.

The Euler-Lagrange equations and the Noether currents are derived from variational principles which are applied to the NLD Lagrangian containing higher order derivatives of the spinor fields  $\Psi$  and  $\bar{\Psi}$ . The generalized Euler-Lagrange equations read [53] ( $\phi = \Psi, \bar{\Psi}$ )

$$\begin{aligned}\frac{\partial \mathcal{L}}{\partial \phi} - \partial_{\alpha_1} \frac{\partial \mathcal{L}}{\partial (\partial_{\alpha_1} \phi)} + \partial_{\alpha_1} \partial_{\alpha_2} \frac{\partial \mathcal{L}}{\partial (\partial_{\alpha_1} \partial_{\alpha_2} \phi)} + \dots + \\ (-)^n \partial_{\alpha_1} \partial_{\alpha_2} \dots \partial_{\alpha_n} \frac{\partial \mathcal{L}}{\partial (\partial_{\alpha_1} \partial_{\alpha_2} \dots \partial_{\alpha_n} \phi)} = 0 \quad .\end{aligned}\quad (6)$$

The invariance of the NLD Lagrangian under global phase transformations results in the following Noether current  $J^\mu$  [53]

$$\begin{aligned}J^\mu = & \left[ \frac{\partial \mathcal{L}}{\partial (\partial_\mu \phi)} - \partial_\beta \frac{\partial \mathcal{L}}{\partial (\partial_\mu \partial_\beta \phi)} + \partial_\beta \partial_\gamma \frac{\partial \mathcal{L}}{\partial (\partial_\mu \partial_\beta \partial_\gamma \phi)} \mp \dots \right] \phi \\ & + \left[ \frac{\partial \mathcal{L}}{\partial (\partial_\mu \partial_\beta \phi)} - \partial_\gamma \frac{\partial \mathcal{L}}{\partial (\partial_\mu \partial_\beta \partial_\gamma \phi)} \pm \dots \right] \partial_\beta \phi \\ & + \left[ \frac{\partial \mathcal{L}}{\partial (\partial_\mu \partial_\beta \partial_\gamma \phi)} - \partial_\delta \frac{\partial \mathcal{L}}{\partial (\partial_\mu \partial_\beta \partial_\gamma \partial_\delta \phi)} \pm \dots \right] \partial_\beta \partial_\gamma \phi \\ & + \dots \quad .\end{aligned}\quad (7)$$

Furthermore, the invariance under space-time translations gives the energy-momentum tensor  $T^{\mu\nu}$  [53]

$$\begin{aligned}
T^{\mu\nu} = & \left[ \frac{\partial \mathcal{L}}{\partial(\partial_\mu \phi)} - \partial_\beta \frac{\partial \mathcal{L}}{\partial(\partial_\mu \partial_\beta \phi)} + \partial_\beta \partial_\gamma \frac{\partial \mathcal{L}}{\partial(\partial_\mu \partial_\beta \partial_\gamma \phi)} \mp \dots \right] \partial^\nu \phi \\
& + \left[ \frac{\partial \mathcal{L}}{\partial(\partial_\mu \partial_\beta \phi)} - \partial_\gamma \frac{\partial \mathcal{L}}{\partial(\partial_\mu \partial_\beta \partial_\gamma \phi)} \pm \dots \right] \partial_\beta \partial^\nu \phi \\
& + \left[ \frac{\partial \mathcal{L}}{\partial(\partial_\mu \partial_\beta \partial_\xi \phi)} - \partial_\gamma \frac{\partial \mathcal{L}}{\partial(\partial_\mu \partial_\gamma \partial_\beta \partial_\xi \phi)} \pm \dots \right] \partial_\beta \partial_\xi \partial^\nu \phi \\
& + \dots \\
& - g^{\mu\nu} \mathcal{L} \quad .
\end{aligned} \tag{8}$$

The Euler-Lagrange equations (6) and the Noether theorems (7) and (8) contain now an infinite series of higher order derivatives of the nucleon field.

It was shown in [53] that in mean-field approximation (up to derivatives of the meson fields which in any case vanish in nuclear matter) these infinite series can be resummed exactly. Indeed, the application of the generalized Euler-Lagrange equations (6) to the full Lagrangian density (3) with respect to the field  $\bar{\Psi}$  leads to the following Dirac equation [53]

$$[\gamma_\mu(i\partial^\mu - \Sigma^\mu) - (m - \Sigma_s)] \Psi = 0 , \tag{9}$$

with the selfenergies  $\Sigma^\mu$  and  $\Sigma_s$  given by

$$\Sigma^\mu = g_\omega \omega^\mu e^{\frac{-v^\alpha i \vec{\partial}_{\alpha+m}}{\Lambda}} + g_\rho \vec{\tau} \cdot \vec{\rho}^\mu e^{\frac{-v^\alpha i \vec{\partial}_{\alpha+m}}{\Lambda}} , \tag{10}$$

$$\Sigma_s = g_\sigma \sigma e^{\frac{-v^\alpha i \vec{\partial}_{\alpha+m}}{\Lambda}} . \tag{11}$$

Both Lorentz-components of the selfenergy,  $\Sigma^\mu$  and  $\Sigma_s$ , show a linear dependence with respect to the meson fields  $\vec{\rho}^\mu$ ,  $\omega^\mu$  and  $\sigma$ , as in the standard RMF. However, they contain an additional non-linear dependence on the partial derivatives.

The following Proca and Klein-Gordon equations for the meson fields are obtained

$$\partial_\mu F^{\mu\nu} + m_\omega^2 \omega^\nu = \frac{1}{2} g_\omega \left[ \bar{\Psi} e^{\frac{i \overleftarrow{\partial}_{\alpha+m}}{\Lambda}} \gamma^\nu \Psi + \bar{\Psi} \gamma^\nu e^{\frac{-v^\alpha i \vec{\partial}_{\alpha+m}}{\Lambda}} \Psi \right] , \tag{12}$$

$$\partial_\mu \vec{G}^{\mu\nu} + m_\rho^2 \vec{\rho}^\nu = \frac{1}{2} g_\rho \left[ \bar{\Psi} e^{\frac{i \overleftarrow{\partial}_{\alpha+m}}{\Lambda}} \gamma^\nu \vec{\tau} \Psi + \bar{\Psi} \vec{\tau} \gamma^\nu e^{\frac{-v^\alpha i \vec{\partial}_{\alpha+m}}{\Lambda}} \Psi \right] , \tag{13}$$

$$\partial_\mu \partial^\mu \sigma + m_\sigma^2 \sigma = \frac{1}{2} g_\sigma \left[ \bar{\Psi} e^{\frac{i \overleftarrow{\partial}_{\alpha+m}}{\Lambda}} \Psi + \bar{\Psi} e^{\frac{-v^\alpha i \vec{\partial}_{\alpha+m}}{\Lambda}} \Psi \right] , \tag{14}$$

where Eqs. (12, 13, 14) show a similar form as in conventional RMF ( $\Lambda \rightarrow \infty$ ), except of the highly non-linear structure in the source terms.

### 3. Isospin-asymmetric nuclear matter

We apply now the NLD model to isospin-asymmetric nuclear matter. In the RMF approximation all meson fields are treated as classical fields. In this approximation the spatial components of the vector meson fields vanish. Moreover, only the third component of the  $\rho$ -meson field in isospin space survives. To simplify the notation, the time-like component of the  $\omega^0$  field will be labelled as  $\omega$ . Similar notation holds also for the time-like and third components in Lorentz- and isospin-space, respectively, of the vector-isovector  $\rho_3^0$  field, which will be denoted as  $\rho$ . The baryon density will be labelled as  $\rho_B$ . For the auxiliary vector we choose  $v^\beta = (1, \vec{0})$ . Note that, additional rearrangement terms can appear for different choices of  $v^\beta$  in the NLD formalism. However, they exactly vanish in the mean-field approximation to infinite nuclear matter [53].

The Dirac equation, see Eq. (9), can be solved using the following *ansatz*

$$\Psi(s, \vec{p}) = u(s, \vec{p}) e^{-ip^\mu x_\mu} \begin{pmatrix} p \\ n \end{pmatrix}, \quad (15)$$

where  $s$  and  $p^\mu = (E, \vec{p})$  stand, respectively, for the spin and 4-momentum of the proton ( $p$ ) or neutron ( $n$ ),  $x^\mu$  denotes the space-time coordinate, and  $u$  is the Dirac spinor for positive energy states. The Dirac equation (9) maintains its form in infinite nuclear matter with selfenergies given by

$$\Sigma_i^0 \equiv \Sigma_{vi} = g_\omega \omega e^{-\frac{E_i - m}{\Lambda}} \pm g_\rho \rho e^{-\frac{E_i - m}{\Lambda}}, \quad (16)$$

$$\Sigma_{si} = g_\sigma \sigma e^{-\frac{E_i - m}{\Lambda}}. \quad (17)$$

The upper (lower) sign in Eq. (16) refers from now on always to protons,  $i = p$ , (neutrons,  $i = n$ ). The Dirac equation is solved inserting Eqs. (15), (16) and (17) into Eq. (9) for protons ( $i = p$ ) or neutrons ( $i = n$ )

$$\gamma_0 E_i^* \Psi_i = (\vec{\gamma} \cdot \vec{p} + m_i^*) \Psi_i, \quad (18)$$

with the in-medium energy and mass given by

$$E_i^* := E_i - \left( g_\omega \omega e^{-\frac{E_i - m}{\Lambda}} \pm g_\rho \rho e^{-\frac{E_i - m}{\Lambda}} \right), \quad (19)$$

and

$$m_i^* := m - g_\sigma \sigma e^{-\frac{E_i - m}{\Lambda}}. \quad (20)$$

These quantities are related to each other through the dispersion relation

$$E_i^{*2} - \vec{p}^2 = m_i^{*2}, \quad (21)$$

which, because of the  $\rho$ -field, is different for protons and neutrons. The solutions of the Dirac equations for protons and neutrons are found in the usual way

$$u_i(s, \vec{p}) = N_i \begin{pmatrix} \phi_s \\ \frac{\vec{\sigma} \cdot \vec{p}}{E_i^* + m_i^*} \phi_s \end{pmatrix}, \quad (22)$$

with the spin eigenfunctions  $\phi_s$ . The factor  $N_i$  is defined as  $N_i = \sqrt{\frac{E_i^* + m_i^*}{2E_i^*}}$  and normalizes the spinors as follows  $\bar{u}_i(s, \vec{p})\gamma^0 u_i(s, \vec{p}) = 1$  and  $\bar{u}_i(s, \vec{p})u_i(s, \vec{p}) = \frac{m_i^*}{E_i^*}$ .

In nuclear matter the meson field equations of motion read

$$m_\sigma^2 \sigma = g_\sigma \rho_s \quad , \quad m_\rho^2 \rho = g_\rho \rho_I \quad , \quad m_\omega^2 \omega = g_\omega \rho_0 \quad , \quad (23)$$

where the vector-isoscalar  $\rho_0$ , vector-isovector  $\rho_I$  and scalar-isoscalar  $\rho_s$  source terms take the forms ( $\kappa = 2$  is the spin degeneracy factor)

$$\begin{aligned} \rho_s &= \sum_{i=p,n} \langle \bar{\Psi}_i e^{-\frac{E_i-m}{\Lambda}} \Psi_i \rangle = \frac{\kappa}{(2\pi)^3} \sum_{i=p,n} \int d^3p \frac{m_i^*}{E_i^*} e^{-\frac{E_i-m}{\Lambda}} \Theta(p - p_{F_i}) = \rho_{sp} + \rho_{sn} \quad , \\ \rho_0 &= \sum_{i=p,n} \langle \bar{\Psi}_i \gamma^0 e^{-\frac{E_i-m}{\Lambda}} \Psi_i \rangle = \frac{\kappa}{(2\pi)^3} \sum_{i=p,n} \int d^3p e^{-\frac{E_i-m}{\Lambda}} \Theta(p - p_{F_i}) = \rho_{0p} + \rho_{0n} \quad , \\ \rho_I &= \sum_{i=p,n} \langle \bar{\Psi}_i \gamma^0 \tau_3 e^{-\frac{E_i-m}{\Lambda}} \Psi_i \rangle = \rho_{0p} - \rho_{0n} \quad . \end{aligned} \quad (24)$$

Contrary to the Walecka model, in the NLD approach the vector-density  $\rho_0$  is not a conserved nucleon density. Latter one has to be derived from the generalized Noether-theorem, see Eq. (7). Following Ref. [53] the conserved nucleon density after the resummation procedure takes the form

$$\begin{aligned} J^0 \equiv \rho_B &= \sum_{i=p,n} [\langle \bar{\Psi}_i \gamma^0 \Psi_i \rangle \\ &\quad - \frac{g_\sigma}{\Lambda} \langle \bar{\Psi}_i e^{-\frac{E_i-m}{\Lambda}} \Psi_i \rangle \sigma + \frac{g_\omega}{\Lambda} \langle \bar{\Psi}_i \gamma^0 e^{-\frac{E_i-m}{\Lambda}} \Psi_i \rangle \omega + \frac{g_\rho}{\Lambda} \langle \bar{\Psi}_i \gamma^0 e^{-\frac{E_i-m}{\Lambda}} \tau_3 \Psi_i \rangle \rho] \quad , \end{aligned} \quad (25)$$

where the expectation value  $\rho_W = \sum_{i=p,n} \langle \bar{\Psi}_i \gamma^0 \Psi_i \rangle$  is just the usual density of the Walecka model [56].

The equation of state (EoS) is obtained from the 00-component of the energy-momentum tensor  $T^{\mu\nu}$ . The resummation procedure described in [53] results in

$$\begin{aligned} T^{00} \equiv \epsilon &= \sum_{i=p,n} \langle \bar{\Psi}_i \gamma^0 E_i \Psi_i \rangle \\ &\quad - \frac{g_\sigma}{\Lambda} \sum_{i=p,n} \langle \bar{\Psi}_i e^{-\frac{E_i-m}{\Lambda}} E_i \Psi_i \rangle \sigma + \frac{g_\omega}{\Lambda} \sum_{i=p,n} \langle \bar{\Psi}_i \gamma^0 e^{-\frac{E_i-m}{\Lambda}} E_i \Psi_i \rangle \omega + \frac{g_\rho}{\Lambda} \sum_{i=p,n} \langle \bar{\Psi}_i \gamma^0 e^{-\frac{E_i-m}{\Lambda}} E_i \tau_3 \Psi_i \rangle \rho \\ &\quad + \frac{1}{2} (m_\sigma^2 \sigma^2 - m_\omega^2 \omega^2 - m_\rho^2 \rho^2) \quad , \end{aligned} \quad (26)$$

with the additional expectation values

$$\begin{aligned} \rho_s^E &= \sum_{i=p,n} \langle \bar{\Psi}_i E_i e^{-\frac{E_i-m}{\Lambda}} \Psi_i \rangle = \frac{\kappa}{(2\pi)^3} \sum_{i=p,n} \int d^3p \frac{m_i^*}{E_i^*} E_i e^{-\frac{E_i-m}{\Lambda}} \Theta(p - p_{F_i}) \quad , \\ \rho_0^E &= \sum_{i=p,n} \langle \bar{\Psi}_i E_i \gamma^0 e^{-\frac{E_i-m}{\Lambda}} \Psi_i \rangle = \frac{\kappa}{(2\pi)^3} \sum_{i=p,n} \int d^3p E_i e^{-\frac{E_i-m}{\Lambda}} \Theta(p - p_{F_i}) \quad , \\ \rho_I^E &= \sum_{i=p,n} \langle \bar{\Psi}_i E_i \gamma^0 e^{-\frac{E_i-m}{\Lambda}} \tau_3 \Psi_i \rangle = \rho_{0p}^E - \rho_{0n}^E \quad . \end{aligned} \quad (27)$$

The pressure  $P$  is given as usual by

$$P = \frac{1}{3} (T^{xx} + T^{yy} + T^{zz}). \quad (28)$$

However, since in the NLD approach rearrangement terms do not appear [53], thermodynamic consistency is always fulfilled. Then, the pressure can be obtained from the energy density by using the thermodynamic relation

$$P = \rho_B^2 \frac{\partial (\epsilon / \rho_B)}{\partial \rho_B}. \quad (29)$$

Note that in Eq. (29) the conserved baryon density  $\rho_B$  from Eq. (25) appears, and not the standard Walecka density.

Two important effects appear in NLD model, which are absent in the minimal  $\sigma\omega\rho$ -models. At first, the selfenergies depend not only on density, but also explicitly on single-particle energy, as discussed in detail in Ref. [53]. These feature is retained also in isospin-asymmetric nuclear matter. As an additional novel feature of the NLD model, not only the Lorentz-vector component of the nucleon selfenergy, but also its Lorentz-scalar part depends implicitly (through the dispersion relation) on the isovector  $\rho$ -meson field. This feature arises from the isospin dependence of the single-particle energy, and it will generate an in-medium mass splitting between protons and neutrons in isospin asymmetric matter. Note that the  $\sigma$  field is also affected by isospin effects, but the residual impact of the dispersion relation is negligibly small in this case.

#### 4. Numerical realization

The meson-field equations depend explicitly on the baryon density, but only implicitly on the single-particle energy. Latter quantity is integrated out in the source terms. Therefore, it is sufficient to solve selfconsistently only the coupled set of meson-field equations (23) at a given density, and then determine the proton or neutron single-particle energy by solving numerically the dispersion relation (21) for a given proton or neutron momentum relative to the nuclear matter at rest.

For the density dependence we proceed as follows: the input parameters are the Fermi-momentum and the isospin-asymmetry. The isospin-asymmetry parameter  $\alpha$  is determined according to the standard definition

$$\alpha = \frac{J_n^0 - J_p^0}{J_n^0 + J_p^0}. \quad (30)$$

The set of the meson field equations (23) is solved then selfconsistently until convergence is achieved. For each iteration step the integrals in Eq. (24) are evaluated numerically, where at each momentum step the dispersion relation, see Eq. (21), has to be calculated also numerically. The whole procedure provides the meson-fields, with which we calculate the corresponding conserved baryon density according Eq. (25) and the isospin-asymmetry



parameter according Eq. (30). Note again, that the conserved baryon density  $\rho_B$  differs from the Walecka one  $\rho^W$ . Finally, the single-particle energies, which appear explicitly in the selfenergies, are evaluated at the corresponding proton or neutron Fermi-momentum.

For the energy dependence at a fixed baryon density the procedure is similar as outlined above. We first calculate the meson-fields at a given density and isospin-asymmetry. Then we solve numerically the dispersion relation for protons (neutrons). In the first case the additional input parameter is the proton (neutron) momentum by keeping the momentum of the other isospin state at the corresponding fixed Fermi-momentum. The in-medium energy of a proton ( $i = p$ ) or neutron ( $i = n$ ) is defined then as

$$E_i = \sqrt{m_i^{*2} + p^2} + \Sigma_{vi} \quad , \quad (31)$$

where the proton or neutron Lorentz-vector selfenergy is given by Eq. (16).

In principle, the NLD model contains no parameters. The original isoscalar  $\sigma NN$  and  $\omega NN$  couplings can be taken from any linear Walecka model, e.g., [55], as it has been done in Ref. [53] and in this work. The  $\rho NN$  coupling  $g_\rho = 3$  close to its universal value is used [60] which is also well determined by the one-boson-exchange model [58]. A small (big) numerical value of  $\Lambda$  provides a stronger (weaker) density and energy dependence of the mean-field, which influences the density dependence of the equation of state for densities at and above saturation and, at the same time, strongly affects the energy dependence of the Schrödinger-equivalent optical potential at saturation density. The simplest way followed here is to fix  $\Lambda$  just from the empirically well-known energy dependence of the Schrödinger equivalent optical potential. The cut-off parameter  $\Lambda$  is set to 770 MeV [53]. A different numerical value for the cut-off parameter is of course possible if one uses a different Walecka-like parametrization than the original one or if one adopts a different functional form for the non-linear operator than the simpler exponential one.

## 5. Results and discussions

Before presenting the calculations for isospin asymmetric nuclear matter we discuss briefly the NLD results for the special cases of symmetric matter ( $\alpha = 0$ ) and pure neutron matter ( $\alpha = 1$ ). In Fig. 1 we present the EoS for  $\alpha = 0$  and  $\alpha = 1$  in terms of the pressure density as function of the baryon density. Here we compare the empirical heavy-ion data [61], see the shaded bands in Fig. 1, with NLD and Walecka models. The inserted panels in Fig. 1 shows the nuclear EoS in terms of the binding energy per nucleon. The conventional Walecka model (dashed curves) leads to a very stiff EoS for symmetric nuclear matter and also pure neutron matter with a high compression modulus at saturation, because of the well-known linear divergent behaviour of the repulsive  $\omega$  field. On the other hand, the Lorentz-vector mean-field is suppressed to large extend at high baryon densities in the NLD model. See further discussions in Ref. [53]. This effect, which is retained also for the extreme case of pure neutron matter, weakens considerably the stiffness of the high-density EoS, see the insert in Fig. 1, and the empirical region in the pressure-density phase diagram is reproduced fairly well by the NLD approach (solid curve).

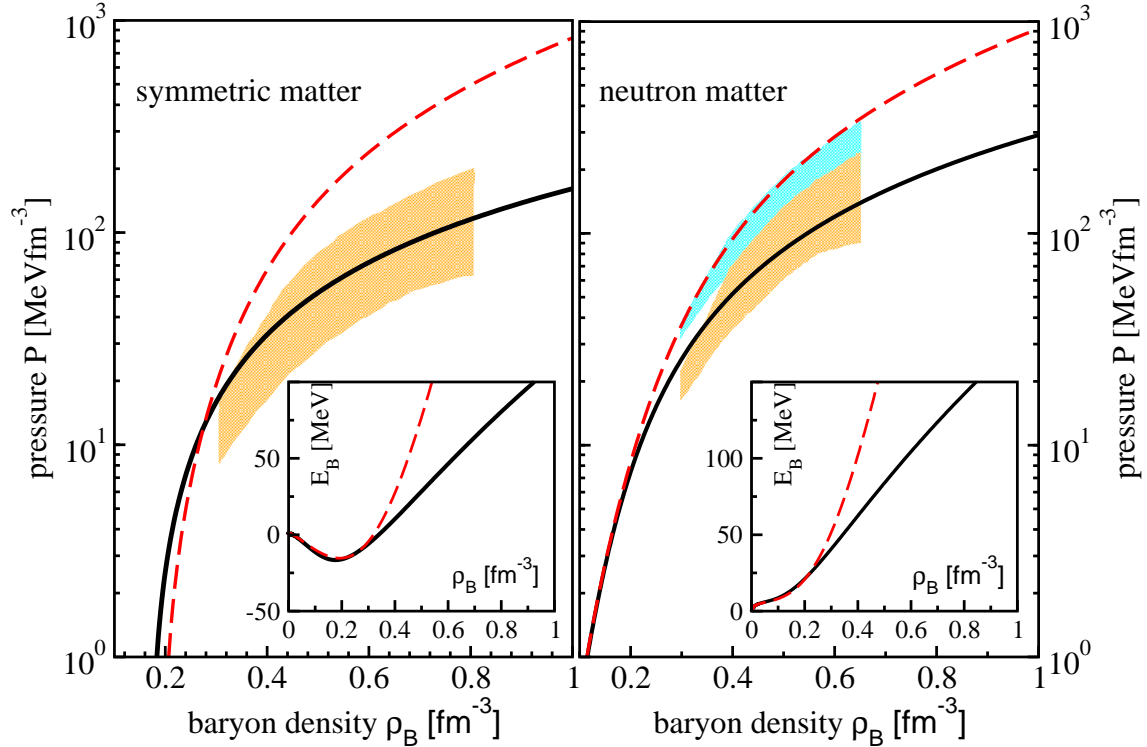


Figure 1: The nuclear EoS for symmetric nuclear matter (main panel on the left) and pure neutron matter (main panel on the right) in terms of the pressure density in the Walecka (dashed curve) and NLD (solid curve) models. The shaded bands refer to the experimental regions extracted from heavy-ion collisions [4, 61]. The inserted panels on the left (right) describe the nuclear EoS for symmetric matter (left) and neutron matter (right) in terms of the binding energy per nucleon  $E_B = \epsilon/\rho_B - m$ , again for both NLD and Walecka models.

However, not only the density dependence of the nuclear mean-field, but also its energy dependence matters for nuclear reactions. This can be demonstrated using the in-medium optical potential which is defined as follows

$$U_{\text{opt}} = \frac{E}{m} \Sigma_v - \Sigma_s + \frac{1}{2m} (\Sigma_s^2 - \Sigma_v^2) . \quad (32)$$

As shown in Fig. 2, the empirical data from Dirac phenomenology (open diamonds) predict a saturation of the in-medium nucleon optical potential [42] at intermediate energies. As well known, standard Walecka-type RMF models (RHD, dashed curve) are not able to reproduce this empirical saturation, and strongly overestimate the data at high energies. This disagreement remains also in other RMF models (DD, dot-dot-dashed curve), where the meson-nucleon couplings depend explicitly on the baryon density. A better description can be achieved here by the consideration of additional energy dependent terms in the interaction Lagrangian (D<sup>3</sup>C, dot-dashed curve). However, with the cost of many additional parameters [37]. Microscopic DBHF models (DBHF, dot-dashed-dashed curve) reproduce the optical potential in average up to energies close to pion production threshold [59, 62]. On the other hand, the NLD model (NLD, solid curve) not only softens the EoS at high densities, but simultaneously generates the correct energy behaviour of the nucleon-nucleus optical potential at high energies. Note that, the same NLD approach describes the puzzling energy dependence of the antiproton-nucleus potential, see Ref. [54].

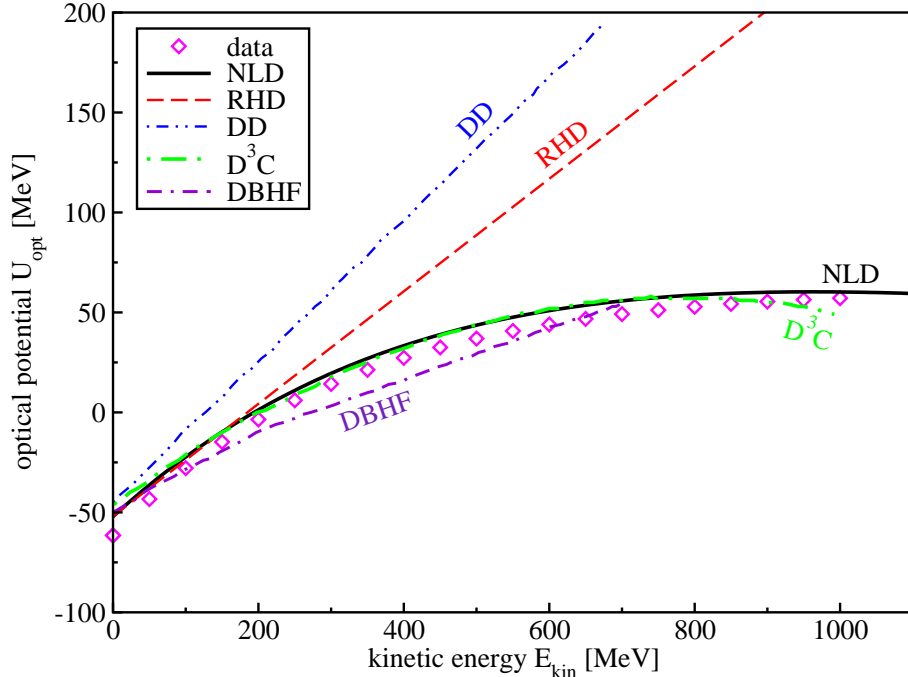


Figure 2: Kinetic energy dependence  $E_{kin} = E - m$  of the Schrödinger equivalent optical potential at ground state density  $\rho_{sat} = 0.16 \text{ fm}^{-3}$  in the linear Walecka (RHD, dashed curve) and NLD (solid curve) models. The other theoretical calculations, DD (dot-dot-dashed curve),  $D^3C$  (dot-dashed curve) and DBHF (dot-dashed-dashed curve), are taken from Refs. [37, 62]. All model calculations are compared with data from Dirac phenomenology (open diamonds) [42].

In Fig. 3 we present the density dependence of the nucleon selfenergies for various asymmetry parameters  $\alpha$ . In symmetric nuclear matter ( $\alpha = 0$ ), the NLD vector  $\Sigma_v$  and scalar  $\Sigma_s$  selfenergies (solid curves) saturate at high densities. As one can see, they essentially follow the density dependence of the microscopic DBHF calculations [63] (filled squares). As discussed in detail in [53], this saturation of the selfenergies with increasing density, in particular, of the repulsive vector part, is responsible for a softening of the EoS at high compressions. The saturation in density remains in the general case of isospin-asymmetric nuclear matter, see the dashed ( $\alpha = 0.5$ ) and dot-dashed ( $\alpha = 1$ ) curves in Fig. 3. As a novel feature, not only the vector, but also the scalar component of the nucleon selfenergy gets isospin dependent. The isospin dependence of the scalar selfenergy, observed here, arises from the  $\rho$ -field induced isospin splitting between the in-medium proton and neutron single particle energies. This effect will be discussed in more details later on.

The saturation of the selfenergies in density affects considerably the density dependence of the symmetry energy. The symmetry energy is extracted from the empirical parabolic law and defined as the second derivative of the energy per nucleon versus the asymmetry parameter  $\alpha$ , or as the energy difference between pure neutron matter and symmetric nuclear matter. Fig. 4 (left panel) shows the density dependence of the symmetry energy within the NLD (solid curve) and the Walecka (dashed curve) models. The symmetry energy  $E_{sym} = T_{sym} + V_{sym}$  in the standard RMF grows almost linearly with baryon density. Here the symmetry potential  $V_{sym}$  is proportional to the  $\rho$  field, which increases

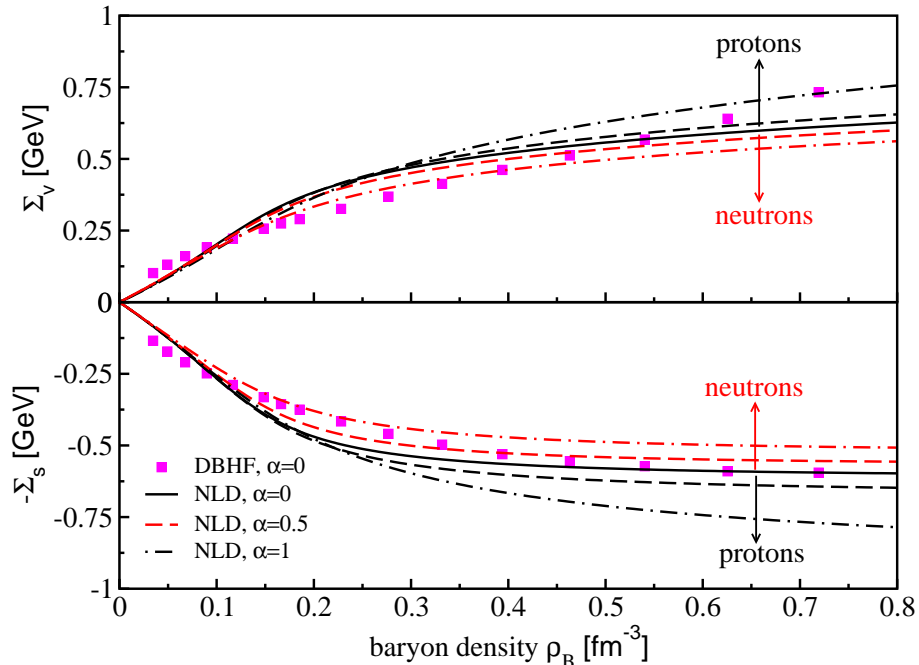


Figure 3: Density dependence of the vector  $\Sigma_v$  (upper panel) and scalar  $\Sigma_s$  (lower panel) selfenergies. The NLD results for symmetric nuclear matter (solid curve) are compared with DBHF calculations [63] (filled squares). The NLD fields for  $\alpha = 0.5$  (dashed curves) and  $\alpha = 1$  (dot-dashed curves) are shown too, and the direction of the proton and neutron splitting is marked by the arrows, as indicated.

linearly with density,  $\rho_B$ . The moderate saturation at very high densities arises from the suppression of the kinetic part  $T_{sym} \sim \frac{\rho^{2/3}}{E_F^*}$  (with  $E_F^*$  being the in-medium Fermi-energy). The NLD model gives a different behaviour at high baryon densities with respect to the conventional RMF. A considerable softening of the high density EoS is obtained, but now for the isovector sector.

Available data for the symmetry energy exist around saturation density only [64]. The theoretical models describe the experimental data fairly well, however, they give different predictions for the high-density symmetry energy, see for reviews Refs. [1, 2]. In non-relativistic models the adjustment of the model parameters to the empirical saturation point does not necessarily constraint the stiffness of the symmetry energy. In fact, a soft and a stiff symmetry energy can be obtained at high densities [2]. In the relativistic Walecka-type models, the high density dependence of the symmetry energy is always stiff [31, 32]. Similar results are obtained in the DBHF approach and within density-dependent relativistic Hartree-Fock (RHF) approaches [40, 41], see the dashed and dot-dot-dashed curves in the right panel of Fig.4, where the symmetry energy becomes stiffer with increasing density [38]. It is interesting to note that the RHF models contains also an energy dependence, apart the density dependent coupling functions. On the other hand, the DD models [34, 37, 36], see the dot-dashed (DD) and dot (DD-ME $\delta$ ) curves in the right panel of Fig.4, predict a rather soft symmetry energy, which is similar to the NLD results (solid curve).

Direct experimental access to the high-density region of the symmetry energy is still

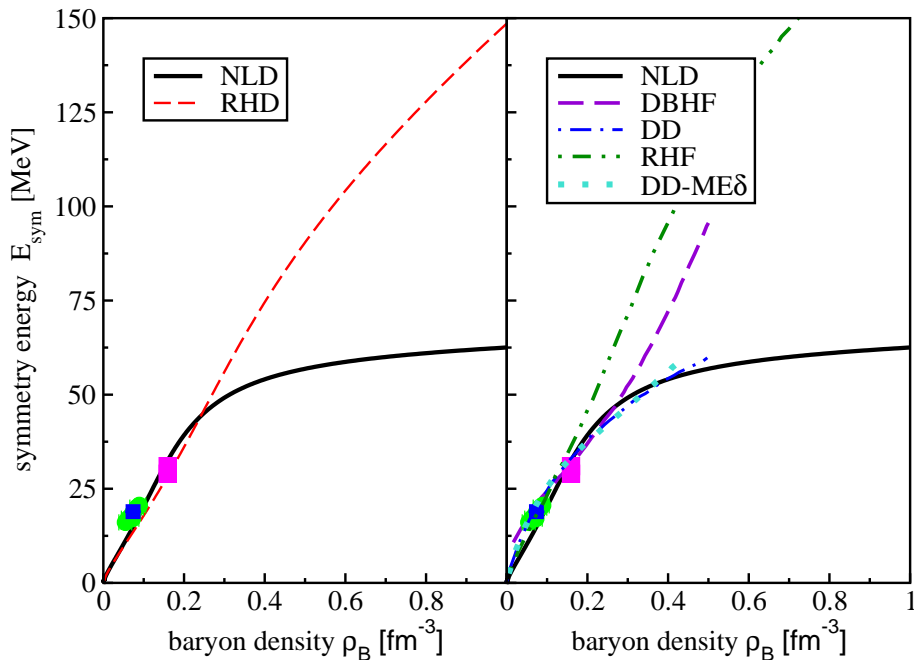


Figure 4: (Left panel) Density dependence of the symmetry energy  $E_{\text{sym}}$  in the standard linear Walecka model (dashed curve) and NLD approach (solid curve). (Right panel) The same as in the left panel, but in comparison between the NLD model with other theoretical approaches: DBHF (dashed curve) [38], DD (dot-dashed curve) [34, 37], RHF (dot-dot-dashed curve) [41] and DD-ME $\delta$  (thick-dotted curve) [36]. The symbols refer to experimental data from Ref. [64].

incompletely known. A plausible way to constraint the stiffness of the symmetry energy at supra-normal densities consists in studies of compact neutron stars [4]. In fact, the symmetry energy must saturate or, at least, show a rather soft behaviour at high baryon densities in order to respect the direct URCA-limit [4]. This constraint is satisfied in the NLD model.

The density dependence of the nucleon effective or Dirac mass in the NLD model [53] is in remarkable agreement with the DBHF calculations. The insert in Fig. 5 describes the Dirac mass of the nucleon in symmetric nuclear matter. Here the solid curve corresponds to the NLD results and the square symbols describe the DBHF calculations of Ref. [63].

Interestingly, in the NLD model an effective mass splitting between protons and neutrons is generated in asymmetric matter by taking into account at the Hartree-level the  $\rho$ -field only. This is demonstrated in Fig. 5 for two asymmetry parameters  $\alpha = 0.5$  (dashed curves) and  $\alpha = 1$  (dot-dashed curves). In particular, a mass splitting  $m_n^* > m_p^*$  is obtained for neutron-rich matter, which becomes pronounced with increasing density and isospin asymmetry parameter. The in-medium mass splitting in the NLD model is due to the isospin dependence of the single particle energy which appears in the selfenergies. Note that, any explicit energy dependence of the scalar selfenergy will result in a  $\rho$ -induced mass splitting of nucleons in isospin asymmetric nuclear matter.

As discussed in the introduction, an effective mass splitting between protons and neutrons do not occur in the Walecka-type  $\sigma\omega\rho$ -models solved at the Hartree-level. The

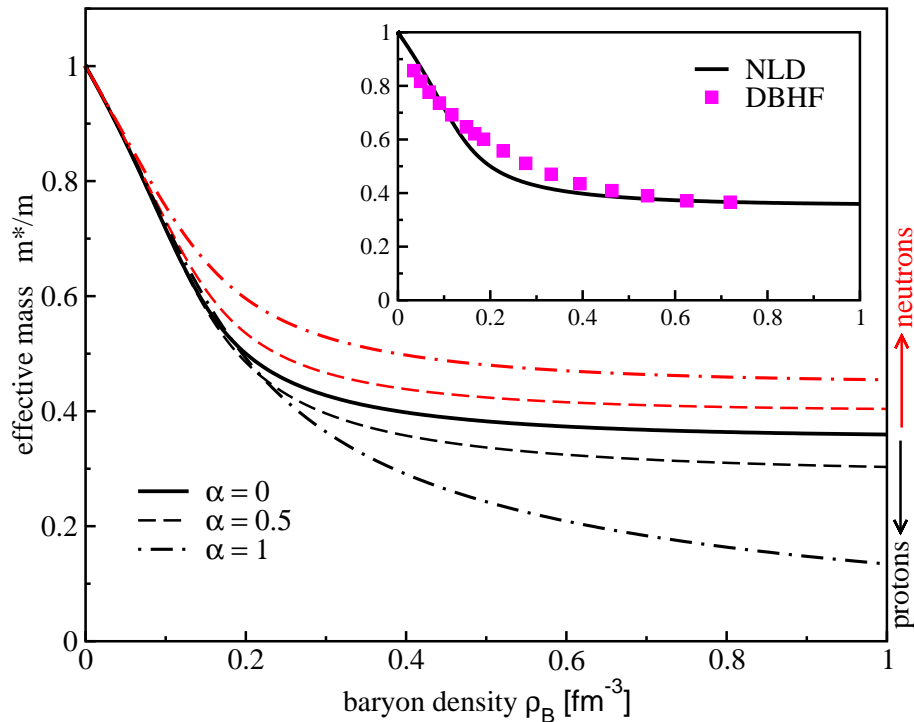


Figure 5: Density dependence of the Dirac mass splitting between protons and neutrons within the NLD model. The asymmetry parameters are  $\alpha = 0$  (solid curve),  $\alpha = 0.5$  (dashed curves) and  $\alpha = 1$  (dot-dashed curve). The curves above (below) the solid curve (symmetric matter) correspond to the neutron (proton) effective masses, as indicated. The insert describes the Dirac mass of the nucleon in symmetric nuclear matter in the NLD (solid) and DBHF [63] (filled squares) calculations.

introduction of the scalar-isovector  $\delta$ -meson in the nuclear mean-field is necessary for this purpose [31, 32]. However, one gets more parameters to fit the bulk asymmetry parameter at saturation density and, in particular, one needs to re-adjust again the  $\rho NN$  coupling. This procedure can be ambiguous, since the  $\delta NN$  coupling is not fixed neither by nuclear structure [34] nor by the one-boson-exchange models [63]. On the other hand, as it has been investigated intensively in the past, the  $\delta$ -meson implies interesting effects if one goes beyond the saturation density of ground state nuclear matter and study its influence in compressed matter created in heavy-ion collisions [24, 25]. Unfortunately, the available experimental data do not allow still decisive conclusions [65]. The  $\sigma\omega\rho\delta$ -models predict a mass splitting  $m_n^* < m_p^*$  for neutron-rich matter [1, 31, 32, 24]. However, just from the energy dependence of the scalar selfenergy the NLD model predicts an opposite splitting  $m_n^* > m_p^*$  for neutron-rich matter. This trend is unique and cannot be reversed in the NLD model. We remind here, that RMF models treated on the Hartree-Fock level (RHF) [40, 41], in which the selfenergies depend also explicitly on the single-particle energy due to the Fock-terms, predict for the non-relativistic effective mass a mass splitting  $m_n^* > m_p^*$  up to densities  $\rho_B < 0.8\rho_{sat}$ , but this trend is reversed for densities  $\rho_B > 0.8\rho_{sat}$  [40]. Therefore, the property  $m_n^* < m_p^*$  is not a genuine feature of the RMF models, as has been believed so far.

The energy dependence of the isovector nuclear potential is described by the Schrödinger-equivalent optical potential, see Eq. (32), but now separated between protons and neutrons.

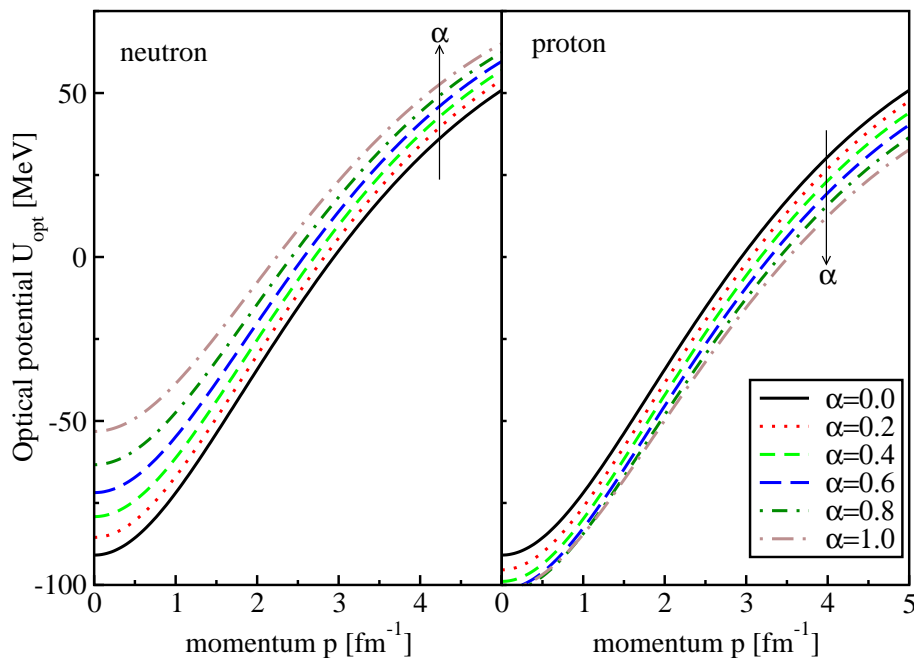


Figure 6: Momentum dependence of the Schrödinger equivalent neutron (left panel) and proton (right panel) optical potentials at various asymmetries, as indicated. Calculations in the NLD model are shown only. The standard RHD model does not contain a momentum dependence.

Fig. 6 shows these potentials as function of the corresponding particle momentum and different asymmetry parameters  $\alpha$ . The observed isospin dependence of the proton (right panel) and neutron (left panel) optical potentials results from cancellation effects in Eq. (32) between different isospin dependent components of the selfenergies. It is remarkable that the microscopic (D)BHF calculations [38, 48, 49] predict very similar behaviour as the NLD model. This is shown in Fig. 7, where the proton and neutron optical potentials are shown as a function of the asymmetry parameter  $\alpha$  at fixed density  $\rho = \rho_{sat}$  and three different momenta, as indicated in Fig. 7. Indeed, at low momenta up to the Fermi momentum (left and middle panels) the isospin splitting between the proton and neutron optical potentials in the NLD model (solid and dashed curves) follows closely the microscopic calculations (filled and open squares for DBHF, filled and open triangles for BHF). At higher momenta (right panel) the NLD isospin splitting is similar to the (D)BHF calculations, up to an absolute value. This is related to a stronger energy dependence in the NLD model relative to these microscopic approaches. Recall, that this strong energy dependence of the NLD potential is essential for the description of the Schrödinger-equivalent optical potential shown in Fig. 2.

The energy dependence of the isovector optical potential is conventionally described by the Lane-type potential. It is defined as follows [1, 2]

$$U_{\text{iso}} = \frac{U_n - U_p}{2|\alpha|}, \quad (33)$$

where  $U_{p,n}$  denotes the proton/neutron Schrödinger-equivalent optical potentials. Fig. 8 shows the momentum dependence of the Lane-potential in the NLD approach (solid curve).

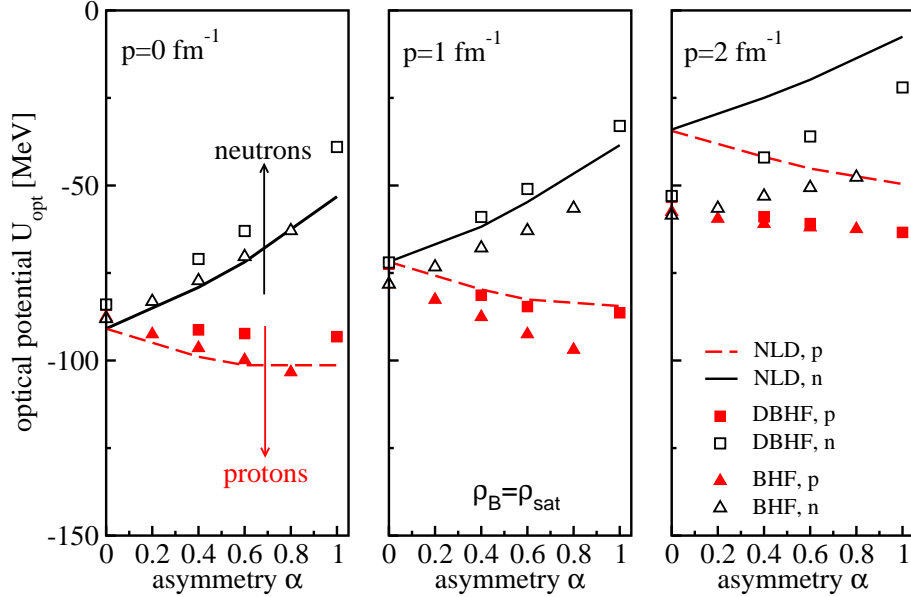


Figure 7: Asymmetry parameter  $\alpha$  dependence of the optical potentials at fixed saturation density and at three fixed momenta ( $p = 0, 1, 2 \text{ fm}^{-1}$  as indicated) in the NLD (solid and dashed curves for neutrons and protons), in the DBHF [38] (filled and open squares for protons and neutrons) and in the BHF [48] (filled and open triangles for protons and neutrons) models. The arrows in the left panel indicate the direction of the proton and neutron splitting in these three figures.

Also the results of linear Walecka model denoted as RHD (dashed curve) and different microscopic approaches are shown. The linear Walecka model predicts an almost linear behaviour in energy, as in the isoscalar case, and it diverges for  $p \rightarrow \infty$ . The Lane potential in the NLD model shows an opposite behaviour with respect to RHD. It decreases with increasing particle momentum. In contrast to the symmetric proton- and antiproton-nucleus optical potentials [53, 54], the empirical situation in the isovector case is still not well known. Different empirical studies predict an opposite behaviour of  $U_{\text{iso}}$  versus momentum. In fact, the analysis of Madland *et al.* [46, 47] predicts an increase of the isovector potential with increasing momentum, while in the analysis of Lane *et al.* [43, 44, 45] a decrease of  $U_{\text{iso}}$  with rising momentum has been obtained. Nevertheless, as shown in Fig. 8, the NLD calculations agree with the calculations from the microscopic Brueckner theory which also show the decrease of the Lane potential as a function of the momentum.

## 6. Summary

In summary, the NLD formalism which incorporates on a mean-field level the energy dependence of the nucleon selfenergies has been applied to isospin-asymmetric nuclear matter. The model describes the bulk properties of symmetric matter and compares well with the results from microscopic Brueckner calculations. Due to the explicit energy dependence of the nuclear mean-field, the NLD model reproduces very well the empirical proton and antiproton optical potentials [53, 54]. Same energy dependence is responsible



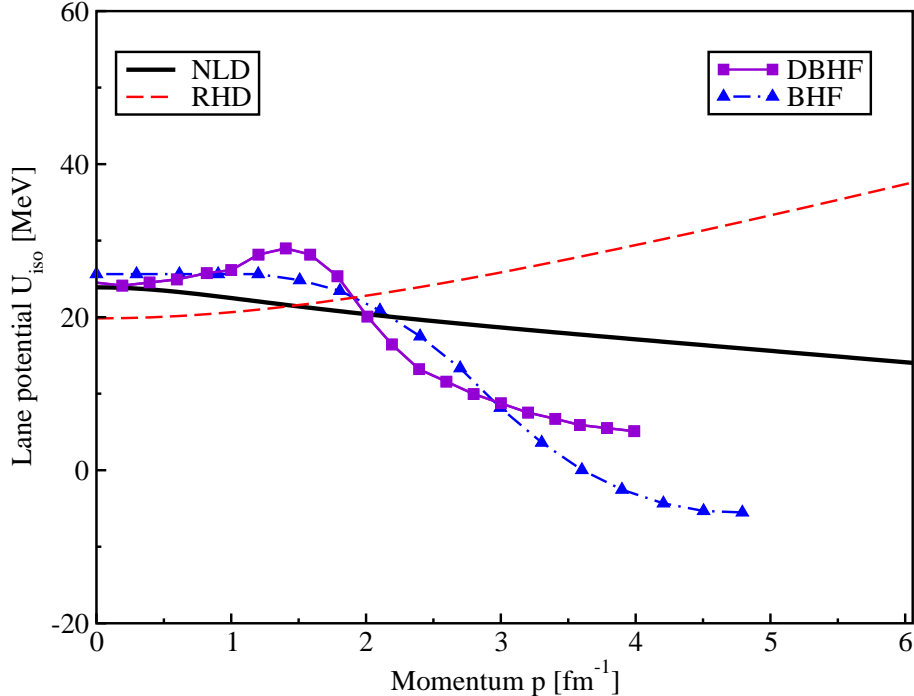


Figure 8: Energy dependence of the Lane potential at saturation density and an isospin asymmetry parameter  $\alpha = 0.4$ . The NLD model (solid curve) is compared with the Walecka model (RHD, dashed curve) and with the DBHF [38] (solid curve with filled squares) and BHF [48, 49] (dot-dashed curve with filled triangles) models.

for the softening of the EoS at high densities. In the present model the isospin effects are generated by using the conventional  $\rho$ -meson exchange. Such a minimal extension of the NLD formalism describes the symmetry energy around saturation and predict its softening (saturation) at high baryon densities. This feature is an important element in the description of dense nuclear systems created in heavy ion collisions and/or in the interior of neutron stars. However, such a soft symmetry energy is at variance with standard RHD models, where it rises linearly with increasing density.

As a novel feature we find that the energy dependent NLD interactions generate a mass splitting between protons and neutrons already within the conventional  $\rho$ -exchange scheme. In particular, a Dirac mass splitting  $m_n^* > m_p^*$  is obtained for neutron-rich matter. However, we point out that the  $\rho$ -induced nucleon mass splitting is a rather general feature of energy dependent interactions and should show up in any model which incorporates them.

We further discussed the energy dependence of the isovector optical potentials. We found that the NLD model leads to a decreasing Lane-type potential with increasing particle momentum. This disagrees with the conventional RMF models, but is consistent with the results from microscopic Brueckner calculations. Also the comparison of the isovector splitting in the proton/neutron optical potentials agrees well with the results from DBHF and BHF microscopic approaches. These suggest that the NLD  $\sigma\omega\rho$  mean-field model which accommodates the energy dependence of nucleon selfenergies, is in qualitative agreement with microscopic (Dirac) Brueckner calculations. Since the NLD model describes also asymmetric matter features fairly well and agrees with microscopic DBHF

models, it could be interesting to apply the NLD approach to finite nuclei. However, due to the energy dependence of the fields, the main advantage of the NLD approach would be its application to the description of heavy-ion reactions within the transport theory.

## Acknowledgments

This work was supported by HIC for FAIR, DFG through TR16 and by BMBF.

## References

### References

- [1] V. Baran, M. Colonna, V. Greco and M. Di Toro, Phys. Rept. **410** (2005) 335.
- [2] B. A. Li, L. W. Chen and C. M. Ko, Phys. Rept. **464** (2008) 113.
- [3] With the term *stiffness* of a quantity one usually refers to its slope at rather high densities in the range  $\rho \simeq (2 - 3) \rho_{sat}$ , where  $\rho_{sat}$  is the density of ground state nuclear matter. A soft (stiff) behaviour of a quantity means then a small (big) slope parameter or a moderate (strong) density dependence of a quantity at supra-normal densities.
- [4] T. Klahn *et al.*, Phys. Rev. C **74** (2006) 035802.
- [5] D. Vretenar, T. Nikšić, P. Ring, Phys. Rev. C **68** (2003) 024310;  
A. Carbone *et al.*, Phys. Rev. C **81** (2010) 041301(R);  
J. Zenihiro *et al.*, Phys. Rev. C **82** (2010) 044611;  
M. Centelles *et al.*, Phys. Rev. Lett. **102** (2009) 122502;  
M. Warda *et al.*, Phys. Rev. C **80** (2009) 024316.
- [6] W. Reisdorf and H. G. Ritter, Ann. Rev. Nucl. Part. Sci. **47** (1997) 663.
- [7] N. Herrmann, J. P. Wessels and T. Wienold, Ann. Rev. Nucl. Part. Sci. **49** (1999) 581.
- [8] P. Danielewicz, Annals Phys. **152** (1984) 305.
- [9] J. Aichelin, Phys. Rept. **202** (1991) 233.
- [10] O. Buss *et al.*, arXiv:1106.1344 [hep-ph].
- [11] W. Cassing, E. L. Bratkovskaya, Phys. Rept. **308** (1999) 65-233.
- [12] G. F. Bertsch and S. Das Gupta, Phys. Rept. **160** (1988) 189.
- [13] H. Stoecker and W. Greiner, Phys. Rept. **137** (1986) 277.
- [14] P. Danielewicz, Annals Phys. **152** (1984) 239.

- [15] W. Botermans and R. Malfliet, Phys. Rept. **198** (1990) 115.
- [16] A. Andronic *et al.* [FOPI Collaboration], Phys. Lett. B **612** (2005) 173.
- [17] C. Fuchs, Prog. Part. Nucl. Phys. **56** (2006) 1.
- [18] L. W. Chen, C. M. Ko and B. A. Li, Phys. Rev. Lett. **94** (2005) 032701.
- [19] D. V. Shetty, S. J. Yennello and G. A. Souliotis, Phys. Rev. C **75** (2007) 034602.
- [20] J. Rizzo, M. Colonna, M. Di Toro and V. Greco, Nucl. Phys. A **732** (2004) 202.
- [21] V. Giordano *et al.*, Phys. Rev. C **81** (2010) 044611.
- [22] B. A. Li, Phys. Rev. C **69** (2004) 064602.
- [23] B. A. Li, Phys. Rev. Lett. **85** (2000) 4221.
- [24] T. Gaitanos *et al.*, Nucl. Phys. A **732** (2004) 24.
- [25] G. Ferini *et al.*, Phys. Rev. Lett. **97** (2006) 202301.
- [26] V. Prassa *et al.*, Nucl. Phys. A **832** (2010) 88.
- [27] Q. f. LI, Z. x. LI, E. g. Zhao and R. K. Gupta, Phys. Rev. C **71** (2005) 054907.
- [28] K. Weber *et al.*, Nucl. Phys. A **539** (1992) 713.
- [29] P. Danielewicz, Nucl. Phys. A **673** (2000) 375.
- [30] P. K. Sahu *et al.*, Nucl. Phys. A **640** (1998) 493.
- [31] S. Kubis and M. Kutschera, Phys. Lett. B **399** (1997) 191.
- [32] B. Liu *et al.*, Phys. Rev. C **65** (2002) 045201.
- [33] C. Fuchs, H. Lenske and H. H. Wolter, Phys. Rev. C **52** (1995) 3043.
- [34] S. Typel and H. H. Wolter, Nucl. Phys. A **656** (1999) 331.
- [35] T. Niksic *et al.*, Phys. Rev. C **66** (2002) 024306;  
G.A. Lalazissis *et al.*, Phys. Rev. C **71** (2005) 024312;  
W.-H. Long, N. Van Giai, S.-G. Zhou, Phys. Rev. C **69** (2004) 034319.
- [36] X. Roca-Maza, X. Vinas, M. Centelles, P. Ring, P. Schuck, Phys. Rev. C **84** (2011) 054309.
- [37] S. Typel, Phys. Rev. C **71** (2005) 064301.
- [38] E. N. E. van Dalen, C. Fuchs and A. Faessler, Phys. Rev. C **72** (2005) 065803.

- [39] E. N. E. van Dalen, C. Fuchs and A. Faessler, *Eur. Phys. J. A* **31** (2007) 29.
- [40] Wen-Hui Long, Nguyen van Giai, Jie Meng, *Phys. Lett. B* **640** (2006) 150.
- [41] Bao Yuan Sun, Wen-Hui Long, Jie Meng, U. Lombardo, *Phys. Rev. C* **78** (2008) 065805.
- [42] E. D. Cooper, S. Hama, B. C. Clark and R. L. Mercer, *Phys. Rev. C* **47** (1993) 297.
- [43] A. Lane, *Nucl. Phys.* **35** (1962) 676.
- [44] J. P. Jeukenne, A. Lejeune and C. Mahaux, *Phys. Rev. C* **10** (1974) 1391.
- [45] A. J. Koning and J. P. Delaroche, *Nucl. Phys. A* **713** (2003) 231.
- [46] R. Kozack and D. G. Madland, *Phys. Rev. C* **39** (1989) 1461.
- [47] R. Kozack and D. G. Madland, *Nucl. Phys. A* **509** (1990) 664.
- [48] W. Zuo *et al.*, *Phys. Rev. C* **72** (2005) 014005.
- [49] W. Zuo, I. Bombaci and U. Lombardo, *Phys. Rev. C* **60** (1999) 024605.
- [50] M. Jaminon, C. Mahaux, *Phys. Rev. C* **40** (1989) 354.
- [51] D. Alonso and F. Sammarruca, *Phys. Rev. C* **67** (2003) 054301.
- [52] F. Sammarruca, W. Barredo and P. Krastev, *Phys. Rev. C* **71** (2005) 064306.
- [53] T. Gaitanos, M. Kaskulov and U. Mosel, *Nucl. Phys. A* **828** (2009) 9 [arXiv:0904.1130 [nucl-th]].
- [54] T. Gaitanos, M. Kaskulov and H. Lenske, *Phys. Lett. B* **703** (2011) 193 [arXiv:1105.4450 [nucl-th]].
- [55] H. P. Duerr, *Phys. Rev.* **103** (1956) 469.
- [56] B. D. Serot and J. D. Walecka, *Int. J. Mod. Phys. E* **6** (1997) 515.
- [57] T. Maruyama, *et al.*, *Nucl. Phys. A* **573** (1994) 653.
- [58] R. Machleidt, K. Holinde and C. Elster, *Phys. Rept.* **149** (1987) 1.
- [59] B. Ter Haar and R. Malfliet, *Phys. Rept.* **149** (1987) 207.
- [60] M. M. Kaskulov, U. Mosel, [arXiv:1103.2097 [nucl-th]]; M. M. Kaskulov, U. Mosel, *Phys. Rev.* **C81** (2010) 045202.
- [61] P. Danielewicz, R. Lacey and W. G. Lynch, *Science* **298** (2002) 1592.

- [62] L. Sehn, C. Fuchs and A. Faessler, Phys. Rev. C **56** (1997) 216.
- [63] R. Brockmann and R. Machleidt, Phys. Rev. C **42** (1990) 1965.
- [64] D. V. Shetty, S. J. Yennello and G. A. Souliotis, Phys. Rev. C **76** (2007) 024606  
[Erratum-ibid. C **76** (2007) 039902].
- [65] X. Lopez *et al.* [FOPI Collaboration], Phys. Rev. C **75** (2007) 011901.